New insights in the use of a strong cationic resin in dye adsorption

Paola Santander, Estefanía Oyarce and Julio Sánchez

ABSTRACT

The adsorption of methyl orange (MO) in aqueous solution was evaluated using a cationic polymer (Amberlite IRA 402) in batch experiments under different experimental variables such as amount of resin, concentration of MO, optimum interaction time and pH. The maximum adsorption capacity of the resin was 161.3 mg g^{-1} at pH 7.64 at 55 °C and using a contact time of 300 min, following the kinetics of the pseudo-first-order model in the adsorption process. The infinite solution volume model shows that the adsorption rate is controlled by the film diffusion process. In contrast, the chemical reaction is the decisive step of the adsorption rate when the unreacted core model is applied. A better fit to the Langmuir model was shown for equilibrium adsorption studies. From the thermodynamic study it was observed that the sorption capacity is facilitated when the temperature increases.

Key words | dyes, pollution, polymers, remediation, resins, water

Paola Santander
Centro de Biotecnología,
Universidad de Concepción,
Concepción,
Chile
and
Núcleo Milenio sobre Procesos Catalíticos hacia la Química Sustentable (CSC),
Santiago,
Chile

Estefanía Oyarce
Julio Sánchez (corresponding author)
Departamento de Ciencias del Ambiente,
Facultad de Química y Biología,
Universidad de Santiago de Chile, USACH,
Casilla 40, Correo 33, Santiago,
Chile
E-mail: *julio.sanchez@usach.cl*

INTRODUCTION

Water pollution is one of the largest and most important problems of our time. There are a variety of pollutants in aqueous environments that can produce serious health effects in plants, animals and humans. These contaminants can be of organic (e.g., dyes, pharmaceuticals, pesticides, etc.) or inorganic (e.g., heavy metals) origin (Vakili *et al.* 2014; Saxena *et al.* 2020).

Dyes are difficult to treat because of their synthetic origin and complex molecular structure, which makes them more stable and difficult to be biodegraded (Forgacs *et al.* 2004; Rai *et al.* 2005).

Some dyes are toxic and mutagenic, and they have the potential to release carcinogenic species. Because of their toxic properties, dyes can also contribute to the failure of biological processes in wastewater treatment plants (Zahrim *et al.* 2010). The presence of very small amounts of dyes in water, even less than 1 mg L^{-1} for some dyes, is highly visible and undesirable (Crini 2006).

In general, synthetic dyes are widely used in many industries, e.g., textile, paper, leather tanning, food processing, plastics, cosmetics, rubber, printing and dye manufacturing (Sokolowska-Gajda *et al.* 1996; Kabdaşli *et al.* 1999; Wróbel *et al.* 2001; Bensalah *et al.* 2009; Aravind *et al.* 2016). Several classes of synthetic dyes (over 7×10^5 metric tons) are produced worldwide every year for industrial purposes, and approximately 5–10% of this quantity is released into the ecosystem along with wastewater. Because of increasingly stringent restrictions on the organic content of industrial effluents, it is necessary to eliminate dyes from wastewater before discharge. One type of dye, methyl orange (MO), which is anionic, has applications in different fields, including coloring paper, temporary hair coloring, and dyeing cottons and wools, among others (Robati *et al.* 2016). Various treatment processes, such as coagulation/flocculation, ozonation, membrane filtration, adsorption, chemical oxidation, solvent extraction, and ion exchange have been widely used to eliminate dyes from wastewater (Foo & Hameed 2010; Karadağ & Üzüm 2012; Moradi *et al.* 2014; Allouche *et al.* 2015). Among these proposed methods, adsorption technology is considered to be one of the most effective methods because of its simplicity, high efficiency, flexibility and insensitivity to toxic substances (Qin *et al.* 2016). Various types of sorbents, including activated carbon, silica gel, clay minerals, fly ash and agricultural solid wastes, have been employed as adsorbents for the removal of dyes from wastewater (Mohan *et al.* 2002; Yan *et al.* 2006; Gómez *et al.* 2007; Wang & Peng 2010; Salleh *et al.* 2011; Chen *et al.* 2012). In the literature, some

doi: 10.2166/wst.2020.158

studies on the removal of dyes using synthetic-based polymer materials have been reported. These materials are for example an ammonium-functionalized hollow polymer (Qin *et al.* 2016) a polyaniline-based nanotube (Ayad & El-Nasr 2010), a polymer-loaded bentonite (Li *et al.* 2010), an ionic-liquid-based cross-linked polymer (Gao *et al.* 2013), quaternary ammonium polyethylenimine (Liu *et al.* 2013), and poly(acrylic acid–acrylamide) hydrogels (Li *et al.* 2011) among a few others. However, the literature is limited to some few polymers and dyes. More research should be done to evaluate well the performance.

Considering the scarce information about the use of commercial resins in dye removal, the aim of this work is to contribute with new information about the use of this kind of resin in the adsorption of sulfonated azo dyes. In this study, we use a commercial cationic resin Amberlite Chloride (IRA 402), a strong cationic resin, to remove methyl orange (MO) dye using the batch method under different conditions such as: amount of resin, MO concentration, and kinetic studies at different pH.

METHODS

Sorption performances of Amberlite Chloride (IRA 402) (Sigma-Aldrich) were examined using the batch adsorption method. MO was purchased from Sigma-Aldrich (85% dye content) and a standard solution of 1,000 mg L^{-1} was prepared and used. For batch adsorption tests, various amounts of resin (15, 30, 50, 75 mg) were contacted with 40 mL of MO solution (20 mg L^{-1} to 200 mg L^{-1}) and stirred to 175 rpm for different times. After that, the resin–MO solution was filtrated and the filtrate was measured in triplicate by UV–vis (Biobase BK560) at 460 nm and the average values of the results were plotted. In the study on the effect of pH, the pH was adjusted using 0.1 mol L^{-1} HCl (Merck) and 0.1 mol L^{-1} NaOH (Merck). For the kinetic study, the interaction times were between 30 and 300 min at 20, 35 and 55 °C in separate experiments. Figure 1 shows the molecular structure of the Amberlite IRA 402 resin adsorbent and MO dye.

The retention percentage (%R) was determined according to Equation (1):

$$\%R = (1 - C_P/C_F) \quad (1)$$

where C_F and C_P are the concentrations of MO in the feed and permeate, respectively. The retention profiles are expressed with the average value.

RESULTS AND DISCUSSION

Batch adsorption of MO on Amberlite IRA 402 resin

A batch test was performed in order to determine the ideal resin amount needed to remove MO. Therefore, different resin loads in a solution of 150 mg L^{-1} of MO at 20 °C and 300 min of contact time were used as initial conditions. The amount of resin was changed from 0.125 to 1.75 g-resin L^{-1}-MO solution. Figure 2 shows that the maximum adsorption of MO was obtained at 119.8 mg MO/g-resin, reaching 99.8% of MO removal. The removal capacity increased when the amount of resin increased until reaching a saturation. This removal can be explained by the attractive interaction between quaternary ammonium groups of polymer and sulfonate groups of MO.

In order to determine the influence of pH on the adsorption capacity of the resin, a study at different pH was performed. The pH studied was 3.00, 7.64 (pH of the MO solution without adjustments) and 10.00. In Figure 3 it is possible to observe that the maximum adsorption is

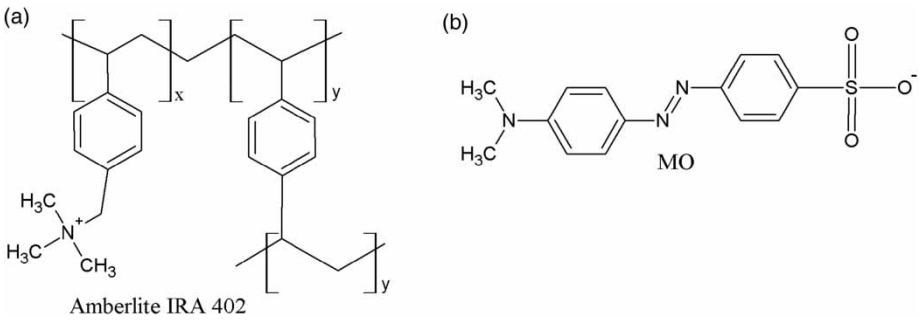

Figure 1 | Molecular structures of (a) Amberlite IRA 402 resin and (b) methyl orange dye.

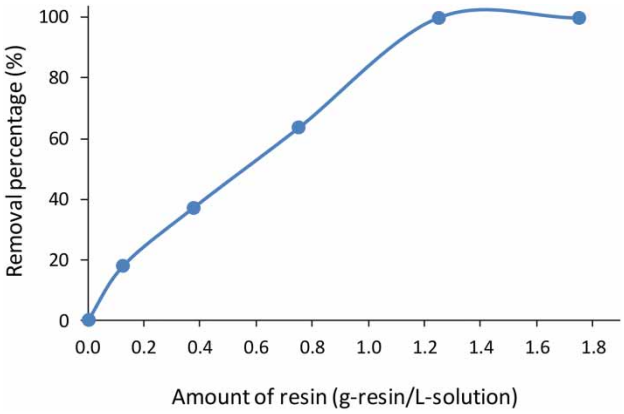

Figure 2 | Effect of resin loading on MO removal (MO = 150 mg L^{-1}, 300 min of contact time at 20 °C).

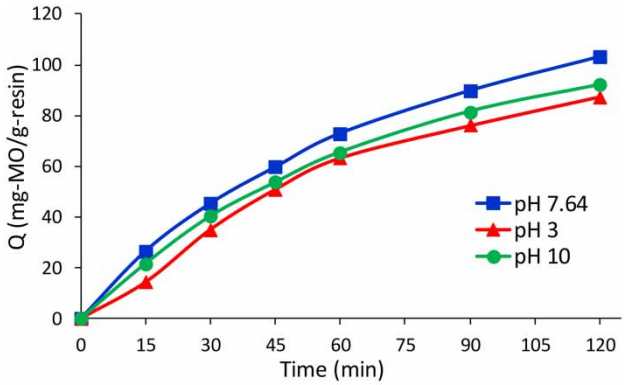

Figure 3 | Influence of the pH on MO removal (MO = 150 mg L^{-1}, resin amount of 1.25 g-resin L^{-1}-solution, 120 min of contact time at 20 °C).

obtained at pH 7.64 under the studied conditions (MO = 150 mg L^{-1}, resin amount of 1.25 g-resin L^{-1}-solution, 120 min of contact time at 20 °C). Thus, this pH was chosen as a working condition in next experiments. The pH of the MO solution affects the adsorption capacity of the resin. The quaternary ammonium groups can interact with MO dye in a wide range of pH due to its low pKa (pKa = 3.4), however at pH 3.00, the removal capacity of the polymeric resin is lower. This is probably due to the protonation of the sulfonate group of the MO, which hinders the attractive interaction between polymer and dye.

Subsequently, a study of the influence of the initial concentration of MO was performed. Resin amount was kept constant while the solution concentration was changed from 50 to 200 mg L^{-1}. Figure 4 shows the adsorption capacity of the Amberlite IRA 402 against each MO concentration. As it is possible to observe, the best adsorption results were obtained at 100 mg L^{-1}, therefore this concentration was used in further experiments. The resin showed

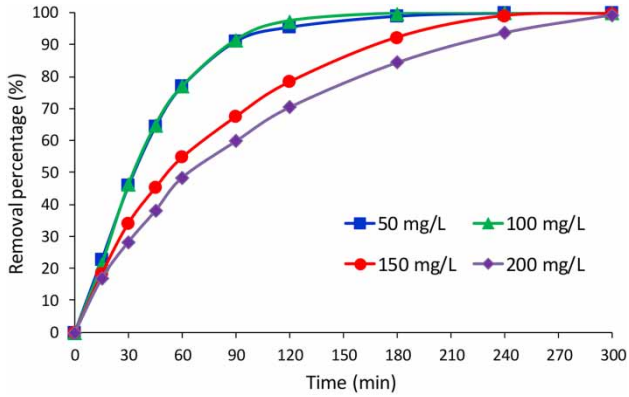

Figure 4 | Removal of MO at different initial concentration as a function of time.

a good adsorption performance at higher MO concentrations (above 100 mg L^{-1}). It can be considered an advantage for dye removal in industrial wastewater treatment due to the wide range of dye concentrations.

In order to study the adsorption performance of the resin, the effect of the temperature as a function of time was analyzed (see Figure 5). As it is possible to observe, the adsorption capacity increases with the increase of the contact time. Under the studied conditions, after 180 min there is no further increase of the sorption capacity, which remains practically constant. Additionally, it is possible to observe that the increase of temperature increases the adsorption capacity, however there are no significant differences in removal capacity at 55 °C and 75 °C.

Based on the experimental data it is possible to establish the best experimental conditions, which are established in Table 1.

Using the best operational conditions, a maximum adsorption capacity of 161.3 mg MO/g-resin was achieved. This result is highly superior to the previous results reported

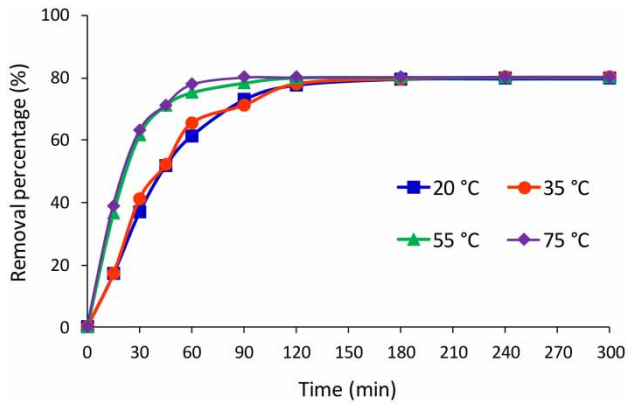

Figure 5 | Influence of temperature and contact time on the MO adsorption capacity of the Amberlite IRA 402.

Table 1 | Best adsorption conditions of Amberlite IRA 402

Parameter	Value
Concentration MO (mg L^{-1})	100
Mass of resin (mg)	50
pH	7.64
Temperature (°C)	55
Contact time (min)	300

in the literature. Leszczyńska & Hubicki (2009) used Amberlite IRA 402 to remove another sulphonated azo dye (brilliant yellow), obtaining a maximum adsorption capacity of 27 mg g^{-1}. On the other hand, Behera *et al.* (2017) used Amberlite IRA 400 to remove MO, obtaining a maximum adsorption capacity of 74.4 mg g^{-1}.

Effect of interfering anions

In this study, the adsorption of MO was evaluated in the presence of anionic species (chloride and sulfate) that compete with the dye, interfering with the adsorption capacity of the resin. The study was performed at different anion/MO molar ratios (see Figure 6). The results show a gradual decrease of the adsorption capacity as the concentration of chloride and sulfate increases when the initial concentration of MO is 100 mg L^{-1} and at a pH of 7.64. The chloride and sulfate anions interact with the resin and this interferes with the level of MO adsorption as the concentration of interfering anions increases, hindering the purpose of the adsorbent and decreasing the adsorption capacity of the resin for the dye. This may be because of the competitive interaction of the MO and the interfering anions with the quaternary ammonium of the resin. In the present study, the influence of interfering anions on MO retention was sulfate > chloride when Amberlite IRA 402 resin was used as adsorbent. However, the resin decreased the removal percentage less than 20% in all the experiments with interfering anions.

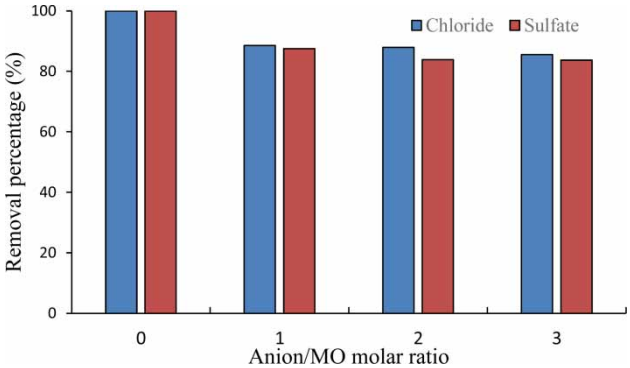

Figure 6 | Effect of interfering anions on the MO adsorption. The adsorption experiments with interfering salts were done in solutions of 100 mg L^{-1} of MO with 50 mg of resin, pH 7.64, 50 °C and a contact time of 300 min.

Similar results have been obtained in previous research related to chromate anion sorption using quaternary ammonium polymer as sorbent and in the presence of chloride and sulfate as interfering anions. The results indicate that when interfering anions were added to the solution, the chromate retention decreased. In general, the concentration, charge, nature of interfering anions, and nature of the functional polymers have effects on its retention capacity. The divalent anions (sulfate) produce a greater reduction than the monovalent anions (chloride) (Sánchez *et al.* 2017).

Kinetic tests

In order to determine some kinetic parameters, some models taken from the literature were used (Guo *et al.* 2005; Yilmaz *et al.* 2007). Equations (2) and (3) show the expressions for pseudo-first and pseudo-second order, respectively:

$$\frac{dq}{dt} = k_1(qe - qt) \tag{2}$$

$$\frac{dq}{dt} = k_2(qe - qt)^2 \tag{3}$$

Integrating and applying the boundary conditions ($qt = 0$ at $t = 0$ and $qt = qt$ at $t = t$) give Equations (4) and (5), respectively:

$$\log(qe - qt) = \log qe - \frac{k_1}{2.303}t \tag{4}$$

$$\frac{t}{qt} = \frac{1}{k_2 q_e^2} + \frac{1}{qe}t \tag{5}$$

where k_1 is the rate constant of pseudo-first order (min^{-1}), k_2 is the rate constant of pseudo-second order (g mg^{-1} min^{-1}) and qe and qt are the adsorbed amounts of MO at equilibrium and at time t (mg g^{-1}), respectively. The correlation coefficients were obtained by plotting log $(qe - qt)$ vs t, for the pseudo-first-order model, and t/qt vs t, for the pseudo-second-order model (Guo *et al.* 2005).

Figure 7 shows the plots for the (a) pseudo-first-order model and (b) pseudo-second-order model at different working temperatures.

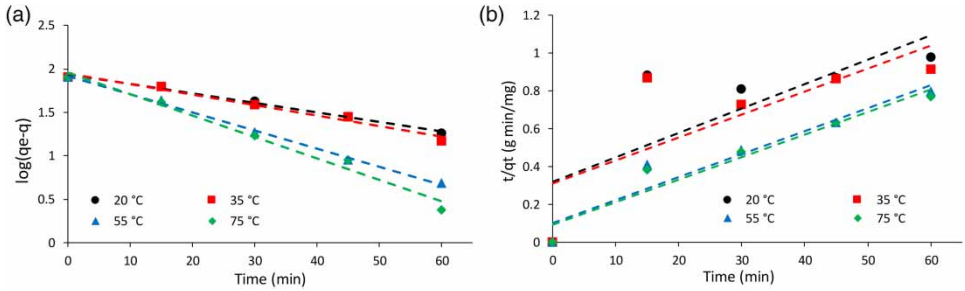

Figure 7 | Plot of (a) pseudo-first-order model and (b) pseudo-second-order model for MO adsorption at different temperatures.

Table 2 shows the kinetic parameters calculated for each temperature. In all the cases the kinetic data fit well with the pseudo-first-order model. As expected, the kinetic constants increase with the increase of the temperature.

To determine the rate-determining steps in the adsorption process, diffusion and reaction models, such as the infinite solution volume (ISV) model and unreacted core model (UCM) equations, were also used. These kinetic models are developed for spherical particles (Yilmaz *et al.* 2007). Table 3 summarizes the ISV and UCM models and Table 4 shows the correlation coefficients for each model at different temperatures.

The ISV model shows that the rate is controlled by the film diffusion process. On the other hand, the chemical reaction is the rate-determining step when the UCM model is applied.

Table 2 | Evaluation of kinetic data of MO adsorption on Amberlite IRA 402 resin according to pseudo-first-order and pseudo-second-order kinetic models

Temperature (°C)	k_1 (min^{-1})	R^2 pseudo-first order	k_2 (g mg^{-1} min^{-1})	R^2 pseudo-second order
20	0.0249	0.990	5.2×10^{-4}	0.588
35	0.0281	0.977	4.8×10^{-4}	0.565
55	0.0477	0.997	1.5×10^{-3}	0.921
75	0.0571	0.983	1.4×10^{-3}	0.932

Table 3 | Diffusion and reaction models

Model	Equation	Rate-determining step
ISV	$-\ln(1-X)=k_t$ where $k=D_rp^2/r_0^2$	Film diffusion
ISV	$-\ln(1-X^2)=\mathrm{K}_{1i}\,t$ where $K_{1i}=3DC/r_0dC_r$	Particle diffusion
UCM	$X=(3C_{A0}K_{mA}/a_{r0}C_{s0})t$	Liquid film
UCM	$3-3(1-X)^{2/3}-2X=(6D_{eR}C_{A0}/a_{r0}2C_{s0})t$	Reacted layer
UCM	$1-(1-X)^{1/3}=(k_sC_{A0}/a_{r0}C_{s0})t$	Chemical reaction

Equilibrium studies

In order to understand the mechanism of the adsorption process, the Langmuir isotherm was used. Owing to some parameters being undetermined for the Freundlich model, a linear behavior was assumed.

The Langmuir isotherm establishes that the adsorption of the adsorbate takes place as monolayer adsorption on the homogeneous surface of the adsorbent. All adsorption sites are equal and the activation energy for the adsorption is uniform for all adsorbed molecules. Equation (6) represents the linear expression of the Langmuir adsorption isotherm (Langmuir 1918):

$$\frac{C_e}{q_e}=\frac{1}{k_lq_l}+\frac{C_e}{q_l} \tag{6}$$

where q_e is the equilibrium adsorption capacity (mg g^{-1}), C_e is the equilibrium concentration of MO (mg L^{-1}), q_l is the Langmuir maximum adsorption capacity (mg g^{-1}), and k_l is the Langmuir constant.

Table 4 | Evaluation of MO adsorption kinetic data according to diffusion and reaction models

	R^2				
	ISV		UCM		
Temperature (°C)	$-\ln(1-X)$	$-\ln(1-X^2)$	X	$3-3(1-X)^{2/3}-2X$	$1-(1-X)^{1/3}$
20	0.989	0.938	0.939	0.962	0.996
35	0.983	0.960	0.902	0.962	0.970
55	0.990	0.991	0.745	0.957	0.929
75	0.968	0.934	0.744	0.976	0.978

Equation (7) represents a linear model of adsorption:

$$q_e = k_l C_e + I \tag{7}$$

where q_e is the equilibrium adsorption capacity (mg g^{-1}), k_l is the linear constant of the process, C_e is the remnant concentration of MO (mg L^{-1}) and I is the intercept. Table 5 shows the calculated parameters for the Langmuir and linear equations.

It seems that the Langmuir model fitted better than the linear model due to the higher correlation coefficient. This result shows that MO adsorption is determined for the homogeneous surface of the adsorbent with sites energetically equivalent.

Thermodynamic studies

The influence of temperature on the adsorption capacity of MO was investigated in order to determine the spontaneity and thermal properties of the adsorption process.

Using the Arrhenius equation (Equation (8)), it is possible to evaluate the values of the activation energy associated with the MO adsorption process. The speed constant used was determined by the pseudo-first-order model (see the section above on 'Kinetic tests').

$$\ln K = \ln A - \frac{E_a}{RT} \tag{8}$$

where K is the rate constant of pseudo-first order (min^{-1}), A is the Arrhenius constant (g min mg^{-1}), E_a is the activation energy (kJ mol^{-1}), R is the ideal gas constant (8.314 J mol^{-1} K^{-1}), and T is the absolute temperature (K). Figure 8 represents the Arrhenius plot of the MO adsorption.

According to the experimental data, activation energy value $E_a = 13.92$ kJ mol^{-1} and correlation coefficient $R^2 = 0.9532$ were obtained. These values could suggest that MO adsorption onto the resin is a physisorption process.

Table 5 | Adsorption isotherm model parameters for MO adsorption on Amberlite IRA 402, 20 °C

Langmuir isotherm			Linear model		
q_l (mg g^{-1})	k_l (L mg^{-1})	R^2	I (mg g^{-1})	k_l (g L^{-1})	R^2
161.3	20.67	0.989	68.18	47.06	0.808

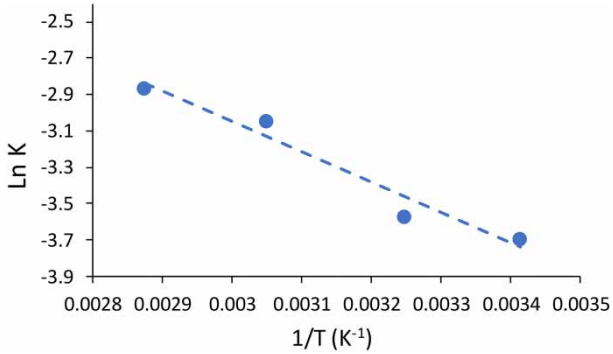

Figure 8 | Arrhenius plot of MO adsorption on Amberlite IRA 402.

The thermodynamic parameters for adsorption of MO by the resin were calculated in order to explain the sorption process. The value of Gibbs free energy was obtained from the Gibbs–Helmholtz equation (Equation (9)) (Pandey *et al.* 2014):

$$\Delta G^o = \Delta H^o - T\Delta S^o \tag{9}$$

where ΔS° is the standard entropy change and ΔH° is the standard enthalpy change. These last parameters can be calculated from the intercept and slope of Equation (10) (Figure 9):

$$\ln K_d = \frac{\Delta S^o}{R} - \frac{\Delta H^o}{RT} \tag{10}$$

where K_d is the distribution constant, obtained by multiplying Langmuir constant K_l and maximum adsorption capacity q_l (mg g^{-1}), R is the universal gas constant (8.314 J mol^{-1} K^{-1}) and T is the absolute temperature (K).

Thermodynamic parameters calculated from the plot are summarized in Table 6. The negative values of Gibbs

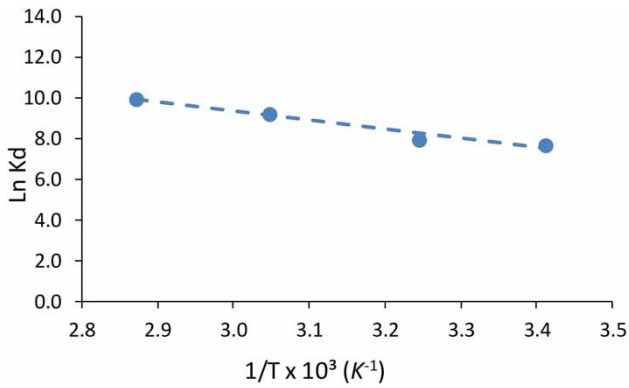

Figure 9 | Plot of ln K_d vs 1/T for MO adsorption on Amberlite IRA 402.

Table 6 | Thermodynamic parameters of MO adsorption on Amberlite IRA 402

	Thermodynamic parameter		
Temperature (K)	ΔG° (kJ mol^{-1})	ΔH° (kJ mol^{-1})	ΔS° (kJ mol^{-1} K^{-1})
293	−18.31	37.18	0.1893
308	−21.15		
328	−24.94		
348	−28.72		

free energy indicate that the MO sorption is of spontaneous nature. It is possible to observe also that the ΔG° value is more negative with increasing temperature, which suggests that higher temperature facilitates the adsorption process. The positive value of ΔH° indicates that the process is endothermic and the positive value of ΔS° indicates a greater stability of the adsorption process with no structural changes at the solid–liquid interface, confirming the spontaneity of the process.

CONCLUSIONS

The present work studied the adsorbent properties of Amberlite IRA 402 on MO removal. It was demonstrated that Amberlite IRA 402 can efficiently remove MO dye. The adsorption capacity is affected by different parameters such as initial concentration, contact time, and temperature, among others. The maximum adsorption capacity of the resin was 161.3 mg g^{-1} at 20 °C, better than the results obtained in previous work for similar studies. Kinetic studies showed that the optimum contact time was 300 min with an optimum temperature of 55 °C. The sorption process follows a pseudo-first-order kinetic model. The rate is controlled by a film diffusion process according to the ISV model and by the chemical reaction, according to the UCM model.

The thermodynamic parameters were also studied. Equilibrium data presented a better fit to the Langmuir isotherm, indicating monolayer sorption. The positive value of activation energy (13.92 kJ mol^{-1}) suggested that the adsorption process was endothermic, and the mechanism was physical adsorption. The values of thermodynamic parameters (ΔG°, ΔH°, ΔS°) were calculated and showed that the adsorption process was endothermic and spontaneous. This resin seems to be a good solution for the removal of this type of dye in wastewater.

ACKNOWLEDGEMENT

The authors thank the FONDECYT Project no. 1191336.

REFERENCES

Allouche, F. N., Yassaa, N. & Lounici, H. 2015 Sorption of Methyl orange from aqueous solution on chitosan biomass. *Procedia Earth Planet Sci.* **15**, 596–601.

Aravind, P., Selvaraj, H., Ferro, S. & Sundaram, M. 2016 An integrated (electro- and bio-oxidation) approach for remediation of industrial wastewater containing azo-dyes: understanding the degradation mechanism and toxicity assessment. *J. Hazard. Mater.* **318**, 203–215.

Ayad, M. M. & El-Nasr, A. A. 2010 Adsorption of cationic dye (methylene blue) from water using polyaniline nanotubes base. *J. Phys. Chem. C* **114** (34), 14377–14383.

Behera, S. S., Das, S., Parhi, P. K., Tripathy, S. K., Mohapatra, R. K. & Debata, M. 2017 Kinetics, thermodynamics and isotherm studies on adsorption of methyl orange from aqueous solution using ion exchange resin Amberlite IRA-400. *Desalin. Water Treat.* **60**, 249–260.

Bensalah, N., Quiroz Alfaro, M. A. & Martínez-Huitle, C. A. 2009 Electrochemical treatment of synthetic wastewaters containing Alphazurine A dye. *Chem. Eng. J.* **149** (1–3), 348–352.

Chen, H., Zhong, A., Wu, J., Zhao, J. & Yan, H. 2012 Adsorption behaviors and mechanisms of methyl orange on heat-treated palygorskite clays. *Ind. Eng. Chem. Res.* **51** (43), 14026–14036.

Crini, G. 2006 Non-conventional low-cost adsorbents for dye removal: a review. *Bioresour. Technol.* **97** (9), 1061–1085.

Foo, K. Y. & Hameed, B. H. 2010 Insights into the modeling of adsorption isotherm systems. *Chem. Eng. J.* **156** (1), 2–10.

Forgacs, E., Cserháti, T. & Oros, G. 2004 Removal of synthetic dyes from wastewaters: a review. *Environ. Int.* **30** (7), 953–971.

Gao, H., Wang, Y. & Zheng, L. 2013 Hydroxyl-functionalized ionic liquid-based cross-linked polymer as highly efficient adsorbent for anionic azo dyes removal. *Chem. Eng. J.* **234**, 372–379.

Gómez, V., Larrechi, M. S. & Callao, M. P. 2007 Kinetic and adsorption study of acid dye removal using activated carbon. *Chemosphere* **69** (7), 1151–1158.

Guo, W. S., Shim, W. G., Vigneswaran, S. & Ngo, H. H. 2005 Effect of operating parameters in a submerged membrane adsorption hybrid system: experiments and mathematical modeling. *J. Membr. Sci.* **247** (1–2), 65–74.

Kabdaşli, I., Tünay, O. & Orhon, D. 1999 Wastewater control and management in a leather tanning district. *Water Sci. Technol.* **40** (1), 261–267.

Karadağ, E. & Üzüm, Ö. B. 2012 A study on water and dye sorption capacities of novel ternary acrylamide/sodium acrylate/PEG semi IPN hydrogels. *Polym. Bull.* **68** (5), 1357–1368.

Langmuir, I. 1918 The adsorption of gases on plane surfaces of glass, mica and platinum. *J. Am. Chem. Soc.* **40** (9), 1361–1403.

Leszczyńska, M. & Hubicki, Z. 2009 Application of weakly and strongly basic anion exchangers for the removal of brilliant yellow from aqueous solutions. *Desalin. Water Treat.* **2**, 160–165.

Li, Q., Yue, Q.-Y., Su, Y., Gao, B.-Y. & Sun, H.-J. 2010 Equilibrium, thermodynamics and process design to minimize adsorbent amount for the adsorption of acid dyes onto cationic polymer-loaded bentonite. *Chem. Eng. J.* **158** (3), 489–497.

Li, S., Zhang, H., Feng, J., Xu, R. & Liu, X. 2011 Facile preparation of poly(acrylic acid–acrylamide) hydrogels by frontal polymerization and their use in removal of cationic dyes from aqueous solution. *Desalination* **280** (1–3), 95–102.

Liu, J., Ma, S. & Zang, L. 2013 Preparation and characterization of ammonium-functionalized silica nanoparticle as a new adsorbent to remove methyl orange from aqueous solution. *Appl. Surf. Sci.* **265**, 393–398.

Mohan, D., Singh, K. P., Singh, G. & Kumar, K. 2002 Removal of dyes from wastewater using flyash, a low-cost adsorbent. *Ind. Eng. Chem. Res.* **41** (15), 3688–3695.

Moradi, O., Norouzi, M., Fakhri, A. & Naddafi, K. 2014 Interaction of removal ethidium bromide with carbon nanotube: equilibrium and isotherm studies. *J. Environ. Health Sci. Eng.* **12**, 17.

Pandey, R., Ansari, N. G., Prasad, R. L. & Murthy, R. C. 2014 Pb(II) removal from aqueous solution by *Cucumissativus* (Cucumber) peel: kinetic, equilibrium & thermodynamic study. *Am. J. Environ. Prot.* **2** (3), 51–58.

Qin, Y., Wang, L., Zhao, C., Chen, D., Ma, Y. & Yang, W. 2016 Ammonium-functionalized hollow polymer particles as a pH-responsive adsorbent for selective removal of acid dye. *ACS Appl. Mater. Interfaces* **8** (26), 16690–16698.

Rai, H. S., Bhattacharyya, M. S., Singh, J., Bansal, T. K., Vats, P. & Banerjee, U. C. 2005 Removal of dyes from the effluent of textile and dyestuff manufacturing industry: a review of emerging techniques with reference to biological treatment. *Crit. Rev. Env. Sci. Technol.* **35**, 219–238.

Robati, D., Mirza, B., Rajabi, M., Moradi, O., Tyagi, I., Agarwal, S. & Gupta, V. K. 2016 Removal of hazardous dyes-BR 12 and methyl orange using graphene oxide as an adsorbent from aqueous phase. *Chem. Eng. J.* **284**, 687–697.

Salleh, M. A. M., Mahmoud, D. K., Karim, W. A. W. A. & Idris, A. 2011 Cationic and anionic dye adsorption by agricultural solid wastes: a comprehensive review. *Desalination* **280**, 1–13.

Sánchez, J., Mendoza, N., Rivas, B. L., Basáez, L. & Santiago-Garcia, J. L. 2017 Preparation and characterization of water-soluble polymers and their utilization in chromium sorption. *J. Appl. Polym. Sci.* **134**, 45355.

Saxena, R., Saxena, M. & Lochab, A. 2020 Recent progress in nanomaterials for adsorptive removal of organic contaminants from wastewater. *ChemistrySelect* **5**, 335–353.

Sokolowska-Gajda, J., Freeman, H. S. & Reife, A. 1996 Synthetic dyes based on environmental considerations. Part 2: iron complexes formazan dyes. *Dyes Pigm.* **30** (1), 1–20.

Vakili, M., Rafatullah, M., Salamatinia, B., Abdullah, A. Z., Ibrahim, M. H., Tan, K. B., Gholami, Z. & Amouzgar, P. 2014 Application of chitosan and its derivatives as adsorbents for dye removal from water and wastewater: a review. *Carbohydr. Polym.* **113**, 115–130.

Wang, S. & Peng, Y. 2010 Natural zeolites as effective adsorbents in water and wastewater treatment. *Chem. Eng. J.* **156** (1), 11–24.

Wróbel, D., Boguta, A. & Ion, R. M. 2001 Mixtures of synthetic organic dyes in a photoelectrochemical cell. *J. Photochem. Photobiol. A: Chem.* **138** (1), 7–22.

Yan, Z., Tao, S., Yin, J. & Li, G. 2006 Mesoporous silicas functionalized with a high density of carboxylate groups as efficient absorbents for the removal of basic dyestuffs. *J. Mater. Chem.* **16**, 2347–2353.

Yilmaz, I., Kabay, N., Yuksel, M., Holdich, R. & Bryjak, M. 2007 Effect of ionic strength of solution on boron mass transfer by ion exchange separation. *Sep. Sci. Technol.* **42** (5), 1013–1029.

Zahrim, A. Y., Tizaoui, C. & Hilal, N. 2010 Evaluation of several commercial synthetic polymers as flocculant aids for removal of highly concentrated C.I. Acid Black 210 dye. *J. Hazard. Mater.* **182**, 624–630.

First received 17 December 2019; accepted in revised form 25 March 2020. Available online 6 April 2020